Bed Ribbing Instability Explanation: Testing a numerical model of ribbed moraine formation arising from coupled flow of ice and subglacial sediment

JOURNAL OF GEOPHYSICAL RESEARCH, VOL. 113, F03005, doi:10.1029/2007JF000954, 2008

Bed Ribbing Instability Explanation: Testing a numerical model of ribbed moraine formation arising from coupled flow of ice and subglacial sediment

Paul Dunlop,[1] Chris D. Clark,[2] and Richard C. A. Hindmarsh[3]

Received 27 November 2007; accepted 1 May 2008; published 24 July 2008.

[1] Ribbed moraines are large (up to 16 km long) ridges of sediment produced transverse to ice flow direction that formed widely beneath palaeo-ice sheets. Since ice sheet stability is sensitive to conditions operating at the bed, an understanding of ribbed moraine genesis will provide critical information on ice sheet dynamics. Currently, there is no consensus on ribbed moraine formation and various competing hypotheses have been presented to account for their genesis. Only one of these theories has been developed into a physically based numerical model that quantitatively describes ribbed moraine formation. This theory, known as the Bed Ribbing Instability Explanation (BRIE), argues that ribbed moraines are produced by a naturally arising instability in the coupled flow of ice and till. BRIE demonstrates that transverse subglacial ridges (i.e., ribbed moraine) spontaneously grow under certain parameter combinations, and it predicts their wavelength (spacing between ridges). The model represents a significant advance because it is the first time a theory of subglacial bedform generation has been developed to make quantitative predictions which can be formally tested. This paper discusses the types of tests that are currently possible and reports the results from the first testing of BRIE. This analysis centers on the ability of BRIE to predict the primary characteristics of ribbed moraine, which are patterning and wavelength. Results show that BRIE successfully predicts the correct ribbed moraine pattern and appropriate wavelengths. The tests fail to falsify the model, and it is concluded that BRIE remains a viable explanation of ribbed moraine formation.

Citation: Dunlop, P., C. D. Clark, and R. C. A. Hindmarsh (2008), Bed Ribbing Instability Explanation: Testing a numerical model of ribbed moraine formation arising from coupled flow of ice and subglacial sediment, *J. Geophys. Res.*, *113*, F03005, doi:10.1029/2007JF000954.

1. Introduction

[2] Ribbed moraines (Figure 1) are prominent landforms which cover extensive areas of the beds of palaeo-ice sheets [*Hättestrand and Kleman*, 1999; *Dunlop and Clark*, 2006a]. Since the late 1800s a wide range of interpretations have been offered which place their formation in a variety of glaciodynamic settings ranging from ice marginal or near marginal positions [*Frödin*, 1913, 1925; *Högbom*, 1920; *Beskow*, 1935] to formation under stagnant ice [e.g., *Lundqvist*, 1951; *Mannerfelt*, 1945; *Kurimo*, 1980]. However, these views have been superseded by the recognition that they formed subglacially [*Hoppe*, 1952; *Lundqvist*, 1969; *Bouchard*, 1989; *Aylsworth and Shilts*, 1989; *Hättestrand and Kleman*, 1999]. This view has important implications for our understanding of ice sheet stability, because the same processes that generate ribbed moraines must logically influence ice sheet motion. Consequently, an understanding of their genesis is of relevance to our knowledge of ice sheet dynamics.

[3] This concept however is complicated by the fact that there is no consensus on their formation. Numerous competing hypotheses have been presented, some of which favor a monogenetic origin, i.e., ribbed moraine are produced by a single formative mechanism [e.g., *Shaw*, 1979; *Bouchard*, 1989; *Aylsworth and Shilts*, 1989; *Fisher and Shaw*, 1992; *Hättestrand*, 1997; *Hindmarsh*, 1998a, 1998b, 1999] while others offer a polygenetic interpretation invoking separate stages of development [*Lundqvist*, 1989, 1997; *Boulton*, 1987; *Möller*, 2006; *Sarala*, 2006]. A longstanding view of ribbed moraines has been that they are initiated by a compressive stress field operating at the glacier sole which acts to shear and stack debris-rich basal ice or basal debris into sequences of subglacial shear planes producing ridges [e.g., *Kurimo*, 1977; *Minell*, 1977, 1980; *Shilts*, 1977; *Shaw*, 1979; *Bouchard*, 1989; *Aylsworth and Shilts*, 1989]. There are differing views on the conditions responsible for generating the stresses and on the glaciodynamic setting of ridge

[1]School of Environmental Sciences, University of Ulster, Coleraine, UK.
[2]Department of Geography, University of Sheffield, Sheffield, UK.
[3]Physical Science Division, British Antarctic Survey, Natural Environment Research Council, Cambridge, UK.

0148-0227/08/2007JF000954$09.00

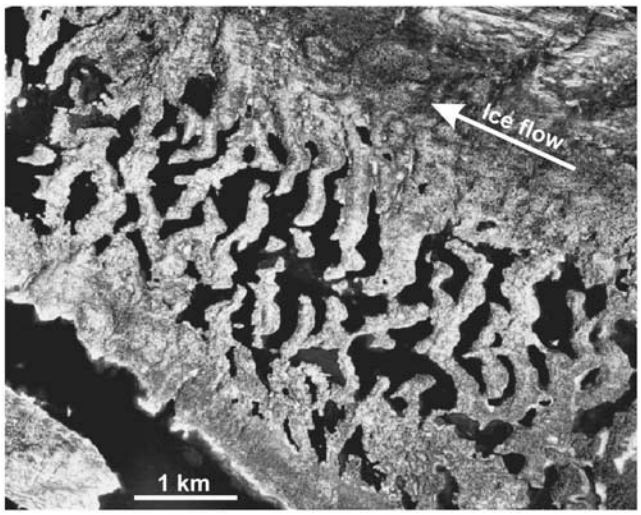

Figure 1. Aerial photograph of classical type ribbed moraine located at Lake Rogen, Härjedalen, central Sweden (62°21′N, 12°24′E). Arrow indicates direction of ice flow.

development. A concise review of the various ideas is given by *Hättestrand and Kleman* [1999]. *Fisher and Shaw* [1992] argue that ribbed moraines are formed by the deposition and reworking of sediments in large ripple cavities that were shaped by subglacial megafloods. *Hättestrand* [1997] suggests a boudinage mechanism whereby a frozen till sheet is fractured and extended into ridges, while others favor a deforming bed mechanism [*Boulton*, 1987; *Hindmarsh*, 1998a, 1998b, 1999]. The polygenetic hypotheses all argue that glacial processes reshape preexisting ridge structures into ribbed moraine ridges. However, there is disagreement regarding the origin of the precursor ridges. *Boulton* [1987] argued that glacial lineations from an earlier glacial stage could act as precursor ridges that would be subsequently reshaped into ribbed moraines following a change of flow direction (through ~90°). *Lundqvist* [1989, 1997] argued the wide variety of sediment and internal structures pointed toward a two-step model, but did not specify the origin of the primary ridges. *Möller* [2006] argues that the precursor ridges were deposited from ice cored moraines in an ice marginal setting. A recent model proposed by *Sarala* [2006] shares similarities with the *Hättestrand* [1997] hypothesis in that the primary ridge structures are produced when a preexisting frozen till sheet is fractured into sequences of protoridges. However, a boudinage mechanism is not favored and an alternative process is proposed in which fracturing is initiated during cold based conditions when ice flow was accommodated by internal deformation. This is thought to initiate a sequence of folds in the basal ice and frozen till sheet which develops into cracks under extensional flow. This continues until the bedrock surface or area of weakness in the drift sheet is intercepted by a rising phase change (melting) surface which promotes sliding at these points and detachment of the ribs.

[4] The theory by *Hindmarsh* [1998a, 1998b, 1999] differs markedly from the above qualitative and case-specific conceptual models in that it is the only quantitative explanation of ribbed moraine genesis. It contains a numerical development of the theory of landform generation by deformable bed mechanisms [*Boulton*, 1987], and models the behavior of an ice sheet sliding over a deforming bed. The theory, herein referred to as the Bed Ribbing Instability Explanation (BRIE), takes a linearized approach and predicts the conditions where amplification of relief in the sediment surface (i.e., landscape formation) can be initiated in deforming subglacial till. The mathematical details and procedures are given by *Hindmarsh* [1998a, 1998b, 1999]. This contribution appears significant because it is the first process-based theory of subglacial bedform generation, in that it incorporates the actual physics required, and which makes predictions that can be quantitatively tested. However, since its formulation in the late 1990s, such testing has not been possible owing to the paucity of data on ribbed moraine characteristics. This shortfall has been recently addressed and there now exists a representative database on ribbed moraine characteristics [*Dunlop and Clark*, 2006a] which can be used to attempt a falsification of the BRIE. Here we introduce the concepts that underpin the theory, describe the model and discuss the types of model tests that are currently possible. Model runs are compared against known ribbed moraine characteristics and an assessment is made on how well the model is able to reproduce the primary features of this landform, and especially with regard to their scale.

2. Instability Mechanisms

[5] It is now well documented that ribbed moraines occur widely over the beds of the former Fennoscandian, Laurentide and Irish ice sheets [e.g., *Prest et al.*, 1968; *Hättestrand*, 1997; *Knight and McCabe*, 1997; *Dunlop and Clark*, 2006a, 2006b]. Recent investigations of ribbed moraines in these regions have established a characteristic and widely repeated patterning, and although the scale of the ridges vary, ridge morphology is fairly consistent between the different ice sheets [*Dunlop and Clark*, 2006a]. Morphometric measures of ridge length, height, width and wavelength (i.e., spacing between ridge center points along the direction of flow) have shown that each parameter has a unimodal distribution and in particular that the ridges have a preferred wavelength within a field [*Dunlop and Clark*, 2006a]. We argue that this consistency in form and pattern, coupled with the unimodal distributions, is indicative of a single formational mechanism which operated widely at the base of these ice sheets. Similar consistency in pattern is common in nature, where there are features that are widespread, repetitive and organized into dominant wavelengths (Figure 2). Such wave pattern formations in natural systems are frequently driven by instabilities (i.e., a mechanism that can amplify small disturbances in the system) and it is well established, for example, in aeolian and fluvial geomorphology, that dunes and other bedforms are created through an instability generated by the interaction of the fluid flow with the underlying bed [e.g., *Hersen et al.*, 2004; *Elbelrhiti et al.*, 2005; *Komarova and Hulscher*, 2000]. Other examples are the Rayleigh-Taylor instability which occurs any time a dense heavy fluid is being accelerated by a light fluid [*Sharp*, 1984], the Kelvin Helmholtz instability which drives some cloud formations [*Drazen*, 2002] and the

Figure 2. (top) Transverse sand ripples formed on a river bed arising from an instability in the coupled flow of water and sand. Note that two wavelengths of bedforms exist presumably resulting from different flow stages of the river. (bottom) Transverse cloud formations organized into dominant wavelength, and also arising from an instability mechanism.

Rayleigh-Bénard instability, which is known to control convection plumes in fluids [*Getling*, 1997]. Since ribbed moraines display pattern characteristics that are similar to other instability phenomena, we argue that the primary mechanism of ribbed moraine genesis is an instability and are simply extending this idea to the flow of ice over a deforming substrate. We essentially appeal to the fact that ribbed moraines look like waves superimposed on the regional topography [see *Clark and Meehan*, 2001, Figure 4], and as they are composed of subglacial material [e.g., *Lundqvist*, 1969; *Shaw*, 1979; *Wattenson*, 1983; *Bouchard*, 1989], that they are produced by an instability mechanism that can amplify small disturbances in the flow, erosion or deposition of till in the subglacial environment.

[6] In nature, any nearly uniform (i.e., not changing significantly with position in at least one of the three possible directions) field is subject to random forcing. Here the term "field" is used to represent a property of the system which varies with position – for example till thickness, sand thickness, air moisture content. Consider sand ripples which are created where sand is being transported by currents. The current is never constant, but varies in time as a result of wave action and wind action. This means that the rate of sediment transport varies in time. The variability of the rate of sediment transport is complicated and we can consider it to be some kind of a random process. For subglacial sediments, the randomness is perhaps due to variations in the till lithology, subglacial water pressure etc.

[7] In the somewhat restricted technical sense used here, a system is unstable when it acts to amplify small disturbances. This means that some manner of positive feedback is operating. If the system is unstable, then small natural variations (perturbations) which occur as a result of the forcing, become larger through the operation of positive feedback, eventually disrupting the near uniformity of the field. For example, on an initially flat sand surface on a beach, a small protuberance (i.e., variation in the sand thickness) encourages local sediment accretion and the protuberance consequently grows. If a pattern or wave is to form, these disturbances must have a preferred horizontal scale, i.e., a wavelength. Such an instability generally grows exponentially with time at least initially and in practice grows fastest at a particular preferred wavelength, called the wavelength of maximum growth rate (Figure 3). This wavelength is determined by the physical operation of the system. There is no absolute principle which says that there must be such a wavelength, but in practice there almost always is – otherwise we would not observe any patterns. For example, if the wavelength of maximum growth rate of a sand ripple were larger than the beach, we would see no ripple.

[8] It is a very general property of small perturbations that they grow exponentially with time. As a consequence of the exponential growth, a perturbation with the preferred wavelength soon comes to dominate, and a pattern forms with

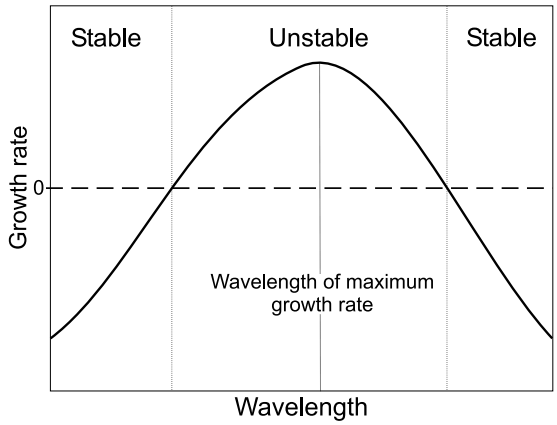

Figure 3. Schematic illustration of the wavelength dependency of instabilities. Graph shows growth rate of instability plotted against wavelength. Where the growth rate is negative, a small perturbation will decay. If there are wavelengths where the growth rate is positive (as illustrated in this example) small perturbations grow in size and the system is unstable. In general the system evolves into a patterned state with a dominant wavelength around the wavelength of maximum growth rate. The detailed physical operation of the system determines the wavelength of maximum growth rate.

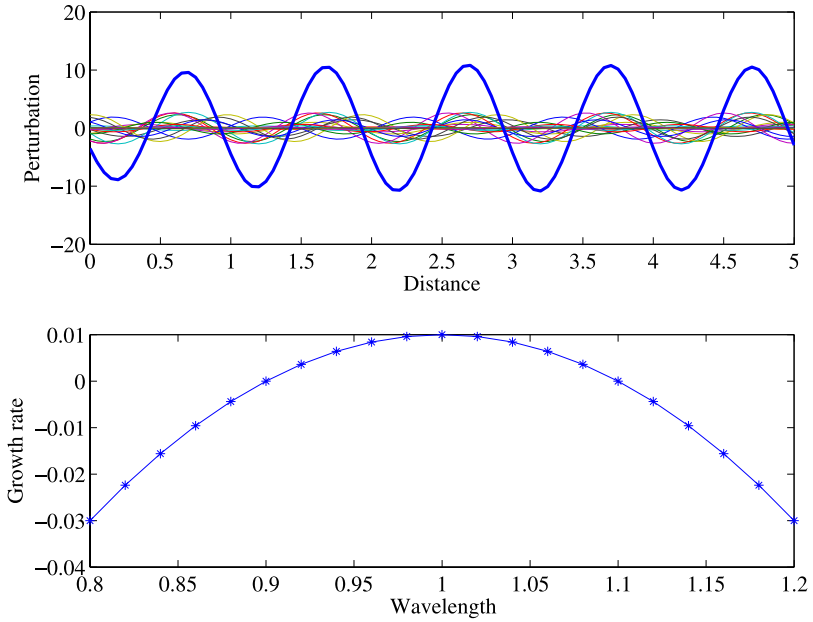

Figure 4. Conceptual illustration of the fact that growth of perturbations at closely related wavelengths produces a net perturbation at a well-defined wavelength. (top) The heavy blue line represents a computed perturbation to an initially flat till surface. Note that the wavelength is around one. (bottom) The growth rate as a function of wavelength. Waves at each of these wavelength are plotted in Figure 4 (top) (multicolored lines) with amplitude given by exp(100 × growth rate), representing their evolution after say 100 years. The heavy blue line in Figure 4 (top) represents the sum of all the multicolored waves. The multicolored smaller waves (the "Fourier components") are not physically observable, only the heavy blue line is directly observable and represents the observed unstable form (i.e., the ribbed moraine).

scales around this wavelength. Eventually, processes that prevent further growth of the instability start to operate, and a new steady patterned form may be reached (see examples in Figure 2). Of course, waves grow at wavelengths other than the wavelength of maximum growth rate, but the net effect of all these waves combined is a wave with wavelength around the wavelength of maximum growth rate (Figure 4).

[9] Several workers have now demonstrated mathematically that instabilities can be generated in subglacially deforming till [*Hindmarsh*, 1998a, 1998b, 1998c; *Fowler*, 2000; *Schoof*, 2007]. This theory joins a large volume of instability theories that have successfully explained patterns in nature [e.g., *Philips*, 1993; *Ashton et al.*, 2001; *Yamamoto et al.*, 2003] and is an appealing idea because it eliminates the requirement for specific localized conditions to be in place before ribbed moraines can be generated. A characteristic feature of instabilities is that they produce the same pattern repeatedly. We would therefore expect an instability that operated in the subglacial zone to manifest itself repeatedly, and in a similar fashion beneath various ice sheets and places. If the system is inherently unstable, then one would expect the instability to operate over large areas of that system.

3. Historical Development of the BRIE

[10] *Hindmarsh* [1998a, 1998b, 1998c] was the first worker to demonstrate mathematically that instabilities can be generated in a deforming bed. The physical basis of this instability stems from the fact that the rheology of till is hypothesized to depend upon the effective pressure. In subglacial till, effective pressure is the amount by which the overburden pressure, due to the overlying ice and sediment, exceeds the pore water pressure and is an index of how strongly the till grains are pushed together. The effective pressure is important in till mechanics because it determines the overall strength of the sediment. As effective pressure decreases, the till becomes less cohesive, allowing more frequent and rapid episodes of deformation. The effective pressure is also affected by the pressure exerted on the till by the flowing ice. To add a greater degree of realism, the theory was extended to include sliding at the ice/till and till/bed interfaces [*Hindmarsh*, 1999]. *Fowler* [2000] using the same physical principles as *Hindmarsh* [1998a, 1998b, 1998c] also demonstrated the existence of such an instability. Both *Hindmarsh* [1998a, 1998b, 1998c] and *Fowler* [2000] suggested that drumlins were formed as the result of the instability, but this was a somewhat optimistic extrapolation of their theories, which at that time had only considered two-dimensional plane flow (i.e., unidirectional flow in the direction of the main ice flow or longitudinal flow). In consequence, they had only demonstrated the instability operated for transverse features, i.e., ribbed moraine. This was confirmed by *Schoof* [2007] who explicitly demonstrated that transverse features, i.e., ridges oriented transverse to flow grow faster than any other shape with a shorter-transverse dimension, for example,

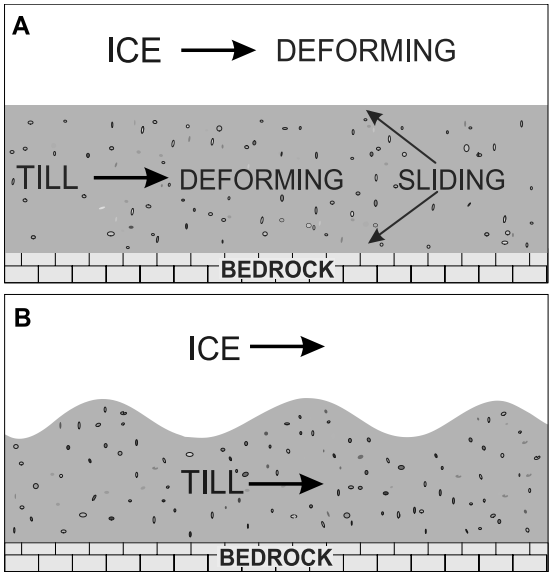

Figure 5. (a) Cartoon of BRIE ingredients. Ice and till can deform internally and sliding can occur at the ice/bed till/bedrock interface. (b) Within certain ranges of parameter space, perturbations can preferentially grow and a wave is initiated in the till.

drumlinoid features, and therefore become the dominant feature. The conclusion from this is that as the instability starts to operate, till waves form and these transverse features will form at around the wavelength of maximum growth rate. In short, *Hindmarsh* [1998a, 1998b, 1998c] and *Fowler* [2000] were premature to regard the instability as a likely cause of drumlins and the mathematical analysis by *Schoof* [2007] demonstrates that the instability might be an explanation for ribbed moraine. However, the possibility remains that model extensions might produce a drumlin forming instability.

4. Description of the BRIE

[11] BRIE is a physically based ice and till flow model that models the behavior of an ice mass coupled to a deforming bed. The physical environment considered is a viscous layer of ice overlying a layer of viscous till which in turn overlies rigid bedrock. Deformation can occur both within the ice and the till, and sliding can also occur at the ice/bed and till/bedrock interface (Figure 5). The bedrock cannot deform. It has been demonstrated that the coupled flow of ice and till is conditionally unstable if bumps exist in the till surface [*Hindmarsh*, 1998b, 1998c; *Fowler*, 2000]. In principle, these bumps can be microscopic, in practice we are supposing that they are sufficiently small not to be recognizable as a precursor landform, and that they do not contain a dominant wavelength. Here, wavelength refers to the horizontal scale of a disturbance in the till thickness. Under certain conditions in BRIE, small undulations in till thickness can grow, causing relief to appear spontaneously. This has been shown to occur over a range of wavelengths [*Hindmarsh*, 1998a]. As explained above, since the instability grows exponentially with time, the growth at the preferred wavelength soon comes to dominate, and a wave forms with length scales characterized by this wavelength.

[12] BRIE self consistently computes stress and velocity fields in ice and till, ensuring that mass is conserved and that forces (momentum) balance – in other words, Newton's Laws are respected. For example, the till pushes back on the ice with a force equal to that which the ice exerts on the till. BRIE uses these principles along with the viscous relationships for till and for ice to predict the variation of velocities and stresses in relation to bump geometry within the ice and the till. The velocities within the till determine whether till bumps grow or decay. Intuitively one can expect physical parameters such as the ice velocity to affect the rate of growth or decay of bumps. BRIE does not use approximations like the shallow ice approximation [*Hutter*, 1983] or higher-order models [e.g., *Blatter*, 1995]; it solves the full system of mechanical equations as did, for example, *Nye* [1969].

[13] The equations (see later) are nonlinear and cumbersome to solve. A significant gain in tractability is gained by assuming that deviations from uniformity in the till and the ice are small compared to till thickness. This at least permits us to predict the wavelength at which landforms will form. Consequently, BRIE can only be used to predict the wavelength at which subglacial landforms are "seeded," i.e., creating an obstacle that generates a feedback, which leads to further growth of the obstacle. Once the bumps become large the predictions of BRIE become inaccurate and the results can be no longer relied upon, although it is unlikely that the wavelength will change dramatically. In more technical terms the nonlinear equations are linearized, and this procedure is no longer accurate when bumps become large. A linearized model deals with a restricted range of bump amplitudes, over which the rate of growth or decay of the height of the bump is linearly proportional to the bump amplitude. For example, if the system is unstable then a bump with twice the amplitude will grow twice as fast. With such a methodology, BRIE can predict the dominant wavelength of the amplified perturbations. However, it is unable to predict the maximum size to which these bumps can grow. To summarize, this theory interprets ribbed moraine as being a wave-like phenomenon caused by this ribbing instability and offers the first physically based explanation of ribbed moraine genesis.

5. BRIE Model: Parameters and Outputs

[14] As mentioned previously, *Hindmarsh* [1998a, 1998b, 1998c, 1999] argues for a viscous rheology of the till. In BRIE the relevant parameters are effective pressure at the surface (p_{e0}), shear stress (τ_0), ice velocity (U_0) and till thickness (D_0), rheological index b and the proportion of ice slip velocity due to till deformation (as opposed to slip of ice over the till). Some of these parameters occur in the rheological relationship

$$\dot{\varepsilon} = A\frac{\tau^b}{p_e^b}, \tag{1}$$

where $\dot{\varepsilon}$ is the strain rate, A is the viscous coefficient of till, τ is the shear stress, p_e is the effective pressure and b is the rheological index. The viscous coefficient A and the index b

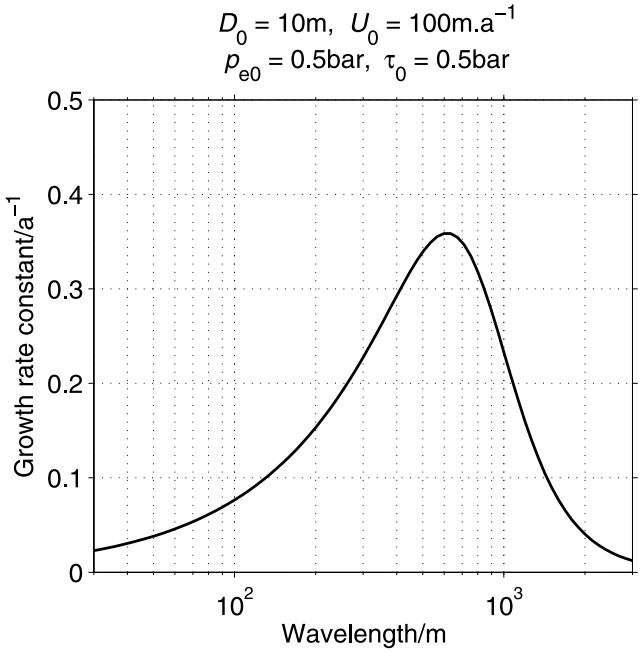

Figure 6. Graphical output of the BRIE showing the dominant wavelength of the instability (solid black line and left axis). In this example a wavelength of 600 m is obtained when the till thickness, D_0 = 10 m, effective pressure ρ_{e0} = 0.5 bar (50 kPa), shear stress, τ_0 is 0.5 bar (50 kPa), and the sliding velocity, U_0 is 100 ma^{-1}. (After *Hindmarsh* [1999].)

are properties of the till, while the shear stress and the effective pressure are determined by the flow of ice and the flow of water in the subglacial hydraulic system.

[15] The rheology of ice is also given by a viscous relationship, the major difference with till being that there is no dependence upon the effective pressure as water pressure within ice is not known to play a significant role in determining its flow. The relationship is of the form

$$\dot{\varepsilon} = B\tau^n, \tag{2}$$

where B is the viscous coefficient for ice and n is another index. The coefficient B is strongly temperature dependent [*Paterson*, 1994], but since BRIE assumes that the bed is at the pressure melting point of ice, we can take a value of B appropriate to that of ice at this temperature. A value of 4.4×10^{-24} Pa^{-3} s^{-1} is used along with the usual glaciological choice of n = 3.

[16] Including a nonlinear rheology is a new feature of the BRIE model and should be compared with the linear rheological relationship used by *Hindmarsh* [1998a, 1998b, 1999], *Fowler* [2000], and *Schoof* [2007]. Use of a nonlinear rheology (n = 3) adds greater realism to the studies. In particular, the viscosity of ice is strongly affected by the shear stress, and this makes a significant difference to the wavelength of maximum growth rate [*Fowler*, 2000]. An analytical solution is still obtainable as the procedure is a linearization. Details will be presented in a future paper.

[17] The viscous coefficient A for subglacial till is poorly understood. However, it has easily computed effects on the mean ice velocity, which is much better constrained. The ice velocity is simply proportional to the parameter A; if this is doubled the ice velocity also doubles, all else being equal. Thus, rather than using the viscous coefficient as a parameter, the ice velocity U_0 is used as a parameter and the viscous coefficient computed from the specified ice velocity, effective pressure, shear stress and the rheological index using the rheological relationship (1) and appropriate formulae for computing the ice velocity from these parameters [e.g., *Hindmarsh*, 1998a, 1998b, 1998c, 1999].

[18] The rheological index b is equally poorly understood. This index determines whether the till deforms viscously or plastically. If b is very large (>10) then the till is effectively plastic. If b is relatively small ($b < 5$), then the till can be regarded as viscous.

[19] Apart from the parameters entering the till rheological relationship, other parameters which affect the characteristics of subglacial instabilities are the till thickness D_0. Account can also be taken of the fact that some of the ice motion can be accommodated by slip at the ice-till interface and also at the till-bed interface. This is represented in the system by specifying the proportion of the ice-sliding velocity taken up by sliding at the ice-bed interface, within the till and at the ice-till interface. Further details are given by *Hindmarsh* [1999].

[20] As mentioned previously, when the model is run, bumps, or instabilities, in the system begin to grow. The instability grows fastest at the preferred wavelength or wavelength of maximum growth rate. The BRIE predicts this dominant wavelength and displays the results in graphical form (Figure 6). In this case, the model predicts a maximum wavelength of around 600 m under the specified parameter settings.

[21] This is gratifying because the data from *Dunlop and Clark* [2006a] indicate that 90 % of ribbed moraine wavelengths lie between 100 m and 1000 m, so the computed wavelength would appear to be very typical. However, this value was obtained for a particular parameter set with D_0 = 10 m, U_0 = 100 m/a, τ = 50 kPa, p_e = 50 kPa, b = 3, and with all the ice velocity accommodated by internal deformation. These are just one set of a very wide range of plausible parameters. In order to be convinced that the theory *can* explain ribbed moraine wavelengths, one needs to determine whether ribbed moraine ridges of the correct wavelength are produced by other plausible parameter values.

6. Approaches to Model Testing

[22] Our reading of the history of subglacial bedform research is that mechanistic case-specific hypotheses have been developed to explain observations from individual or small groups of landforms which may not be representative of the population. Curiously, the naming of bedforming phenomena into discrete and specific landforms (drumlins, ribbed moraine) may have hindered progress as it focuses enquiry and explanation on the specific landform, rather than the complete surface or field. Defining a drumlin, for example, as a specific landform emphasizes it is a bump in a landscape, and the beauty of its streamlined shape, rather that the overall bumpy pattern of a drumlin field. While true understanding of bedforms will require complete explanation of all aspects, we argue that the paramount question and

starting point should be the holistic question of patterning; that is, why does a presumably otherwise flat sheet of sediment become organized such that repetitive and well organized thickenings in this sediment yield a bumpy upper surface that forms a pattern we are able to recognize and name? In this viewpoint we ask what processes change the sediment thickness such that the upper surface resembles bedforms. The explanation thus hinges on relief amplification from a flat surface (bump making) rather than specific forms of individual landforms (bump shaping). Which mechanisms cause bumps to grow, or did selective erosion occur to leave bumps behind? The primary characteristic of a series of well organized and repetitive bumps are their wavelength and amplitude (i.e., organization in space), with shape and symmetry of each form a secondary concern. Much of the bedform literature addresses and seeks explanation of the secondary characteristics (shapes; such as drumlin streamlining or ribbed moraine ridge asymmetry) while the overall patterning characteristics are less well explored. We note that *Smalley and Warburton* [1994] made an appeal to investigate drumlin fields rather than drumlins with the rather elegant argument drawing analogy between bumps on golf balls and drumlin fields. Bumps on golf ball are designed with amplitude and wavelength such that they induce numerous small vortices behind them and which provide less drag through the air than a singular large vortex, and thus a bumpy golf ball travels further than a smooth similarly sized ball. An interesting question is whether ice sheets shape their beds to change its roughness for reasons of flow efficiency.

[23] We regard that a promising theory for the production of subglacial bedforms should first be capable of explaining the geometry of patternings, followed by shaping and other characteristics. Of course any observation that contradicts the theory is capable of falsification, but we propose starting with the primary characteristics. We thus organize our testing procedure around this notion, and in this paper describe how well BRIE performs in explaining ribbed moraine wavelength.

[24] An ideal test would involve controlled physical experimentation (in a constructed ice and sediment "flume") in which input parameters (e.g., ice velocity) are manipulated and bedforms actually grown. The wavelengths of resulting bedforms could be measured to assess the accuracy of theory predictions. If the theory correctly predicts the wavelengths for a whole range of experiments with widely varied values of controlling parameters, then we could conclude it performs well and is probably correct. This is a common approach taken for model testing with regard to aeolian and fluvial bedforms, especially those that are small and form quickly. Such an approach for testing subglacial bedforms however is fraught with difficulty, given the spatial (10^2–10^3 m) and temporal scales (0.1–100s years) of the phenomena in question.

[25] If we cannot manipulate controlled experiments of this environment, another approach is to exploit fortuitous real world situations. For example, for places in Antarctica, if we knew enough about the range of relevant parameters (ice velocity, sediment thickness, effective pressure etc.) and could image the bed using geophysics sufficiently well to identify ribbed moraine, we could use the model to predict in which areas ribbed moraine should be forming and at what wavelength. If for many different places and combinations of governing parameters, the model correctly predicted the occurrence of ribbed moraine and their wavelength we would conclude it is a good model. Unfortunately data do not yet exist for such an approach.

[26] Given that at present we cannot manipulate controlled experiments or exploit real world cases where ribbed moraine are actually forming (we know of no such place) we have to develop tests which do not rely on a direct matching of the controlling parameters with the resulting landforms. The following questions provide first-order tests of increasing power, and as argued earlier we focus on the primary characteristic of ribbed moraine wavelength: (1) Can the model produce a pattern resembling ribbed moraine? (2) Can the model predict ribbed moraine wavelengths over the full range found in nature? (3) Does the model predict the most commonly found wavelengths? (4) Does the predicted length of time for landform generation conform to expectations? (5) Are observed spatial trends in wavelength in nature correctly simulated by the model?

7. Choice of Parameter Values

[27] An important consideration of model testing centers on the parameter ranges used during model runs. To be of any real value, parameter space needs to be adequately constrained so that only sensible values are used. If the model produces sensible results under unrealistic parameter settings it is of no use as a tool in understanding the subglacial environment. Consequently, parameter ranges must be constrained to ensure the values used approximate those that occurred in nature during ribbed moraine formation. If realistic parameter values are used and the model predicts the ribbed moraine characteristics accurately this would bolster the validity of BRIE. Considering that there are many uncertainties regarding the beds of contemporary ice sheets, estimating the exact basal conditions that occurred beneath Pleistocene ice sheets is highly problematic. Nonetheless, by using information from contemporary ice sheets and knowledge regarding ribbed moraine properties and their spatial distribution, we contend that parameter space can be adequately constrained. The following sections outline the logic for choosing the parameter ranges used for this study.

7.1. Till Thickness

[28] The most obvious place to get estimates of till thickness is to investigate the sediment of ribbed moraine fields. However, despite the numerous detailed studies conducted on ribbed moraines there have been few investigations of sediment thickness. *Lundqvist* [1969, 1997] commented that the till sheet between individual ridges is generally thin, and seismic investigations in the Lake Rogen area [*Wattenson*, 1983] have found that most of the surficial material is contained within the ribbed moraine ridges and that the till sheet is thin or lacking in between. These are important observations and help provide some diagnostic clues as to the original thickness of the till sheet before it was deformed. If it is assumed that the situation is similar in the other regions, i.e., that ribbed moraines contain most of the sediment, then ribbed moraine ridges are approximately twice as thick as the till sheet that they originated from. This

is actually a controversial assumption, because it assumes that the instability theory is correct and that waves are being produced. *Dunlop and Clark* [2006a] have reported that ridge heights range from 1 m to 64 m in height. On the basis that the original till thickness was half the ribbed moraine height, the lower limit for the till thickness parameter is taken as 0.5 m and the upper value 30 m.

7.2. Shear Stress

[29] BRIE requires that mean stress be a parameter. This should not be confused with the local stress, which fluctuates around any subglacial obstacle. The mean stress can be equated with the basal shear stress as commonly defined in glaciology. In simple terms, basal shear stress in glacial systems is due to both the weight of the overlying ice and the slope of the ice surface. For small bed slopes, the shear stress at a point can be calculated from the following equation:

$$\tau = \rho_i g h \sin \alpha, \tag{3}$$

where τ is the shear stress, ρ is the density of ice, g is gravitational acceleration, h is the ice thickness and α is the surface slope of the ice. Regarding Pleistocene ice sheets, it is difficult to see how this formula can be of much use as a method for estimating basal shear stress, as all of the components necessary for making the calculation are effectively unknown. Using contemporary ice sheets as an analog is probably a better way of determining the range of shear stress that can occur in nature at the ice sheet scale as all the components of the equation can be measured.

[30] By using equation (3), the basal shear stresses for many valley glaciers have been calculated and estimates show that values vary typically between 50 and 150 kPa [*Paterson*, 1994]. More recent investigations conducted on ice streams resting on deformable sediment show that the driving stresses can be much lower. For example, the driving stress of Ice Stream B in the Siple Coast, Antarctica has been estimated to be 20 kPa [*Alley et al.*, 1989] and as low as 10 kPa [*Jackson and Kamb*, 1997]. Moreover, the flanks of ice streams can support much of this stress, so that the basal stress can be much lower than the driving stress in ice streams [*Whillans and Van der Veen*, 1993]. Values as low as 2 kPa (the cohesive strength of till) have been suggested [*Jackson and Kamb*, 1997]. Inside the main body of the ice sheet shear stresses are much higher with the maximum shear stress being estimated to be 100 kPa [*Paterson*, 1994]. To test the BRIE model, the range of shear stress values is chosen to encompass the range found in ice sheets; 2 kPa to 100 kPa.

7.3. Effective Pressure

[31] The effective pressure enters BRIE through the rheological relationship (equation 1). The effective pressure is a measure of the normal stress that is exerted on the till by the overlying ice sheet. Since BRIE assumes that the pressures within the till are lithostatic and hydrostatic, only the effective pressure at the interface between the ice and the till needs to be specified. This effective pressure is defined by subtracting the pore water pressure from the ice overburden pressure. Since rising pore water pressures reduce the overall shear strength of the till, consequently high values of effective pressure would indicate that the till has a high yield strength, can withstand high shear stresses and is less likely to deform. Low values would signify the opposite, with yield stresses significantly less than that of the overlying ice [*Paterson*, 1994]. Since BRIE presupposes that the till is deforming, there is an implied upper limit to effective pressures, as we need not consider those that increase the strength of the sediment to the point where the till can no longer deform. As a rough approximation to the upper value of effective pressure, we can use Coulomb's Law (equation 2.2) to state that $\tau = \eta p_e$, where η is the coefficient of friction. A typical value for η is 0.5, but it can be as low as 0.25, taking this with the maximum value of the shear stress discussed above (100 kPa) then the largest effective pressure that permits deformation is given by $p_e = \tau/\eta$. This gives a maximum effective pressure of 400 kPa. Even though an argument based on plasticity is being used here, this is consistent with the view of *Hindmarsh* [1997] who argues that viscous deformation is the aggregate of many plastic events. Plastic failure must occur for deformation to occur. Evidence for ponds beneath Ice Stream C implies that the effective pressure can be as low as zero. BRIE assumes that effective pressures are greater than zero, so somewhat arbitrarily the lowest effective pressure is taken as 2 kPa. Thus, a realistic range of effective pressures for a deforming system will range somewhere between 2 and 400 kPa, and these values are used to test the model.

[32] This effective pressure is the value at the ice till interface. Under the assumptions of the model, the effective pressure increases with depth as the weight of the sediment presses the grains harder together. The increase of effective pressure with depth is taken as 10 Pa m^{-1}. This value is justified by *Hindmarsh* [1998a]. It can be seen from equation (2) that the strain rate will depend on the depth of the point being considered beneath the ice-till interface. The shear stress can be considered to be constant over the depth of the till [*Hindmarsh*, 1998a; *Fowler*, 2000]. The additional velocity component of the ice, as a consequence of till deformation is given by summing (integrating) the strain rates over the depth of the till.

7.4. Ice Velocities

[33] Ice sheet velocities are known to vary significantly depending on the position that is being measured. Generally speaking, the slowest moving ice will be found in the interior with velocities at the ice divide being close to zero. The fastest velocities are found in ice streams which are known to vary considerably from around 100 m/a^{-1} (where a is years) for Ice stream B to 12,600 m a^{-1} for Jakobshavn Isbrae [*Joughin et al.*, 2004]. Although ribbed moraines have been identified within palaeo-ice stream tracks [*Dyke et al.*, 1992; *Stokes and Clark*, 2001; *Dunlop*, 2004; *Stokes et al.*, 2006; *Dunlop and Clark*, 2006a] interpretations of their position within the onset zone and superimposition on top of the ice stream bedforms means they are more likely to be associated with the slower ice velocities experienced in onset zones and during ice stream shut down [*Dunlop*, 2004; *Stokes et al.*, 2006]. Since ice velocities involved in ribbed moraine formation will be less than those found typically in fully functioning ice streams, ice velocities will be restricted to those typical of

Table 1. Parameter Values Used to Generate Wavelength Histograms[a]

Parameter	Notation	Units	Values
Basal shear stress	τ	kPa	2,5, 7.5, 10, intervals of 2.5 to 100 (full parameter set) 2,5, 7.5, 10, intervals of 2.5 to 25 (restricted parameter set)
Interfacial effective pressure	P_e	kPa	2, 5, 10, intervals of 5 to 100, 200, 300, 400
Mean velocity	U_0	m/a	0.5, 1, 1.5, 2, 2.5, 3, 4, 5, 6, 8, 10, 15, 20, 25, 30, 45, 60, 80, 100
Rheological index	b		1, 2, 3, 4, 5, 6, 7, 8, 9, 10
Till Thickness	D_0	m	0.5, 0.75, 1, 1.5, 2, 2.5, 3, 4, 5, 6, 8, 10, 20, 30

[a]See Figure 7.

ice sheet flow. For simplicity, we chose the lower and upper values to be 0.5 and 100 m/a^{-1}.

7.5. Rheological Index

[34] As stated previously, the rheological index b parameter is unknown and has been set to either low numbers, i.e., 1–3 (i.e., a viscous rheology) or to high numbers e.g., 10 or more (i.e., a plastic rheology). We consider the range as being 1–10 to encompass both viscous and plastic rheologies. It turns out that the results are not sensitive to this parameter, which fortunately decouples the rheological and geomorphological issues. Table 1 lists the parameter values used for model runs.

8. Results

[35] We now proceed to ask whether the BRIE always, sometimes, rarely or never predicts the formation of ribbed moraine using our justified parameter ranges. Clearly, if it never predicts the formation of ribbed moraine then the model is wrong; however, the other possibilities are more complicated. For example, BRIE may not only predict the range of wavelengths observed, but may also predict ribbed moraines to occur at many other wavelengths not found in nature. Does this mean that the BRIE is wrong, or that the chosen range of parameters is wrong? We have gone to some lengths to give motivation and justification for likely ranges of these parameters, but in our present state of knowledge, it is not possible to constrain them any further. However, we cannot assert that this particular range of parameters is appropriate when ribbed moraines are forming. In general, we would expect a much more restricted range of parameters to have existed during the lifetime of formation of a particular ribbed moraine than the full range used for each parameter.

[36] We can estimate growth timescales for ribbed moraines which are given by the ratio of wavelength to velocity. With wavelengths of a few hundred meters, and ice velocities greater than 1 m a year, this implies ribbed moraine can build up in decades or centuries. We use this estimate to assert that during the time taken to create a ribbed moraine field that ice velocities did not vary greatly. In the same way, one might expect that during the period of formation of a ribbed moraine field, the mean shear stress needs to be constant, because the ice thickness and surface slope would not change much during this period. It is harder to argue that the effective pressure was constant in view of the large fluctuations in water pressure observed in alpine glaciers [*Paterson*, 1994]. However, this is largely a consequence of connection to the outside world (e.g., through crevasses and moulins) and for features formed some distance back from the margin, and thus under thicker ice, effective pressure changes are likely to be inhibited or significantly muted because the pathways for surface meltwater are either closed or would be long. These factors require us to be careful in the conclusions we draw from the comparison of predicted and observed wavelengths.

[37] Figure 7 shows histograms of predicted and observed ribbed moraine wavelengths. The observed results are those reported by *Dunlop and Clark* [2006a], binned logarithmically. The predictions come from populations of computed wavelengths of maximum growth rate, one histogram for the parameter ranges described earlier, the other for a reduced parameter set which was chosen to make the mean predicted and observed values approximately the same – in other words a first attempt to invert for the controlling parameters from the data.

8.1. Can the Model Produce a Pattern Resembling Ribbed Moraine?

[38] This question relates to the primary characteristics of a pattern (e.g., wavelength), rather than the intricate geomorphological details of ribbed moraines such as topographic ridge asymmetry or downstream pointing horns. The ridges that make up a ribbed moraine field resemble simple waveforms (i.e., repetitive ridge spacings). Such a three-dimensional pattern comprising waves must have a dominant downstream wavelength and any lateral wavelength must be much greater than this (otherwise the pattern would not consist of waves). While BRIE does not currently produce map plane outputs (i.e., a three-dimensional surface), it does predict the downstream wavelengths that should arise (see later and Figure 7), and we use the results of *Schoof* [2007] to assert that this is a ribbing instability, in that the lateral (across flow) wavelength is shown to be very large. BRIE predicts a patterning of sediment thickness (i.e., relief amplification to produce landforms) and that this pattern is composed of waveforms (rather than pimples, for example). We thus conclude that at the most basic level, the model produces the right type of pattern. Although a fairly primitive test, we note that competing theories of ribbed moraine genesis [e.g., *Bouchard*, 1989; *Fisher and Shaw*, 1992; *Hättestrand*, 1997; *Möller*, 2006; *Sarala*, 2006] have yet to undergo this test based on a physically formulated model.

8.2. Can the Model Predict Ribbed Moraine Wavelengths Over the Full Range Found in Nature?

[39] Clearly the model would be wrong, or at least incomplete, if it cannot explain the full scale range of ribbed moraine wavelengths. Ribbed moraines are known to exist at a variety of scales, with the smallest, called "minor ribbed moraine," found in Sweden [*Hättestrand*, 1997]

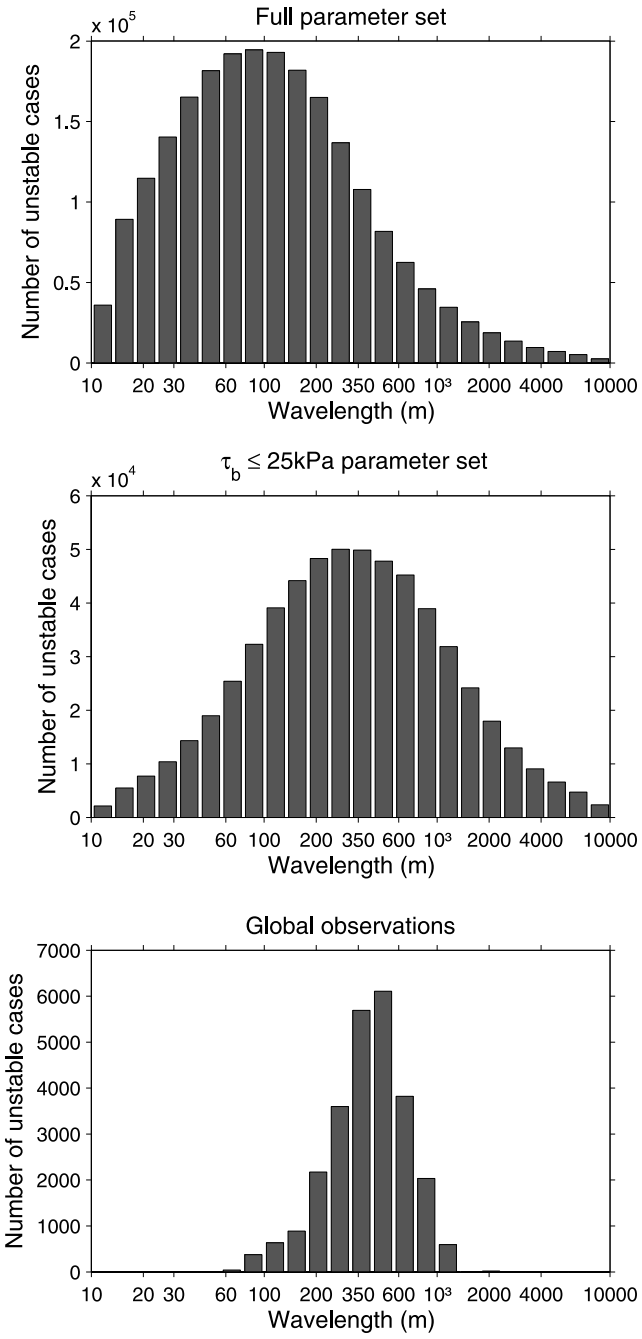

Figure 7. Comparison between the (bottom) measured wavelength and (top and middle) predicted wavelengths. Comparison is through histograms of measured wavelength (Figure 7 (bottom)) or occurrence of predicted wavelength. Predicted populations are generated through computing wavelength as a function of a large number of parameter combinations. Figure 7 (top) is the full parameter set, and Figure 7 (middle) is a reduced parameter set. Full parameter set compiled from 2,116,800 parameter combinations, reduced parameter set complied from 529,200 parameter combinations, and observations based on ribbed moraine wavelength measurements obtained from transects totaling 12,000 km in length.

Ireland and Canada [*Dunlop*, 2004] with wavelengths estimated at less than 100 m, through to the largest, found in Ireland [*Clark and Meehan*, 2001] called "megascale ribbed moraine" with wavelengths estimated between 250 m to 1850 m [*Dunlop*, 2004]. *Dunlop and Clark* [2006a] report a systematic analysis of ribbed moraine wavelengths performed by both manual techniques and spectral (Fourier) analysis on downstream-aligned transects totaling 13,500 km in length, across ribbed moraine fields in Canada, Ireland and Sweden, and encompassing all major ribbed moraine types including minor and megascale. They report a range of wavelengths from 12 to 5800 m. Of the 2116800 model runs thus far produced exploring the full governing parameter space, the predicted wavelengths range between 12 and 8000. This exceeds the range found in nature, and we thus fail to falsify the model. In fact it appears a major achievement to produce a single process formulation that encompasses the whole range of wavelengths measured from minor through to megascale ribbed moraines.

8.3. Does the Model Predict the Most Commonly Found Wavelengths?

[40] The observed frequency distribution of ribbed moraine wavelengths (Figure 7) demonstrates that they are distributed approximately lognormally. The unimodality suggests that it is appropriate to search for a single process theory to explain the whole range of observed ribbed moraine, rather than a collection of different theories to, say, explain minor ribbed moraine and megascale ribbed moraine. If different formative theories were required, one might expect a multimodal wavelength distribution. The most common wavelengths occur around 400 m with around 90% of all ribbed moraine wavelengths found between the ranges of 100–800 m.

[41] A good test of the BRIE would be to see whether it predicts ribbed moraine at the most common wavelengths found in nature; clearly a good theory should be able to reproduce the wavelength frequency distribution, and explain why wavelengths around 400 m are the most common. If one compares the predicted and observed wavelength distributions (Figure 7), a broad similarity in shape is apparent. However, for the model runs using the full parameter range, the modal wavelength is around 100 m, which is less than the observed value of 400 m. What does this mismatch mean; an incorrect model or incorrect choice of parameters?

[42] We show that we can tune the parameter ranges to get a modal value close to the observed value, by restricting the range of mean shear stresses (Figure 7), but such an approach logically invalidates the comparison as a strict "test." It merely shows that the model can produce the appropriate modal wavelengths if we resort to tuning. In general, we caution that comparison of the modal peak positions and distributions should not be taken as a robust or powerful test, because they do not actually compare like with like. This is because we do not have enough information on which particular parameter settings most commonly produced ribbed moraines. For example, when glacial processes produced ribbed moraines at the wavelengths we now observe, the governing parameters had a particular (but unknown to us) probability distribution. Maybe, for example, the landforms preferred to generate under

velocities of 30 ma^{-1} and an ice thickness of 400 m, rather than equally across the whole velocity and ice thickness range. We of course have no means of knowing the parametric probability distribution that operated in the past. Thus for pragmatic reasons we did not use a probability density function, but simply let velocity vary in equal increments across the range from 1 to 100 ma^{-1}, whereas we recognize that in nature it may have varied across this range but with a mode of say 10 ma^{-1}.

[43] An obvious approach around this problem would be to estimate the probability density function for all the governing parameters (velocity, till thickness, shear stress, effective pressure, rheological exponent and deformational velocity proportion), but too little information exists to guide a sensible choice, thus making such an approach rather meaningless. We could of course have tuned the parameter ranges such that the predicted wavelength distribution matches the observed. However, this would not have been a test of the model, but rather would presume the model is correct and be an exploration of the parameter ranges required to produce ribbed moraine. This is an interesting goal for the future, but premature at this stage, since we are currently interested in learning whether the model reasonably works. We should also note that our exploration of parameter space included all permutations, many of which might be glaciologically unfeasible, and that this might help explain why the predicted wavelength distribution is larger than the observed.

8.4. Does the Predicted Length of Time for Landform Generation Conform to Expectations?

[44] This is an important question but we do not have a very strong empirical basis for such expectations. Clearly if the model predicted growth of a ribbed moraine in a matter of seconds, or longer than the lifespan of the ice sheet then the model is wrong. Unfortunately, there is scant guidance from the geomorphological literature as to likely timescales. *Rose* [1989] suggested subglacial bedforms can be created within a period of between 4 and 400 years irrespective of their size. The first observation of bed forming occurring under a contemporary ice mass (Rutford Ice Stream, Antarctica) suggests that an elongated bump, interpreted as a drumlin, grew to a height of 10 m in 7 years under an ice flow velocity of around 400 ma^{-1} [*Smith et al.*, 2007]. However, this velocity is faster than we expect for ribbed moraine generation, which is not associated with streaming ice [*Dunlop*, 2004]. Thus it seems reasonable to expect ribbed moraine generation to occur under slower ice sheet velocities (<100 ma^{-1}) and to take longer periods to form. Since the time frame for development remains essentially unknown, a tentative timescale for development might lie in the range of 10 to 1000 years.

[45] The question has relevance to predicted sedimentary structures found within ribbed moraine, and in particular whether we expect them to be completely composed of till, or of till overlying a core of undisturbed preexistent material. If a ribbed moraine ridge can travel several wavelengths while its relief is increasing, we expect the maximum elevation of the undisturbed parent material to be approximately uniform, corresponding to the depth of the base of the deformation beneath the intercostal trough. If however, the relief builds up in a time where the ridge travels a distance short compared with the wavelength, then we expect that the preexisting material will have been excavated from beneath the trough only, and for the upper surface of undisturbed material to be higher underneath the peaks of the ribbed moraine. While the ribbed moraine has small amplitude compared with the depth of deformation, these effects will be apparent, even though the relief is slowly increasing. It is only then the ribbed moraine amplitude is comparable with the depth of deformation that we expect it to produce observable effects such as we describe above in the geometry of the undisturbed material. Since in the linearized theory the relief grows exponentially, i.e., at a rate proportional to its size, in order to compute the distance traveled while the ribbed moraine is growing, we need to define a starting size. This could be based on the depth of deformation as argued above, but to facilitate comparison we choose a typical depth of deformation (100 mm) and use this as the starting size. Anything smaller and we would not expect to be able to observe the consequences in the internal stratigraphy, while anything larger is no longer a conservative assumption.

[46] Using BRIE we take a 100 mm bump and work out how long it takes to grow into a typically sized ribbed moraine (of 20 m relief). A typical model run provides a growth rate of 0.5 per year (i.e., a factor of $(e)^{0.5}$ per year), which equates a relief amplification of 1.65 of its size each year. For this case it grows into a 20 m bump in approxiamtely 6 years. This appears a reasonable timescale. For the range of growth rates that BRIE derives, the fastest a 20 m bump could grow ranges from less than a year to nearly 10000 years, which are the extreme limits, and may not be realistic.

[47] Given that our theory requires that as a bump grows it also migrates downstream at some fraction of the ice velocity, then an important consideration is whether the ribbed moraine has sufficient time to grow before it emerges at the ice sheet margin. Given that ribbed moraine are generated at large distances from ice margins and grow in times shorter than the residence of time of ice sheets it is clear that bumps can grow quickly enough before being migrated out the system. For the full range of parameter space explored we report the range of times it takes to grow a 20 m high ribbed moraine and the distance they migrated downstream during their growth (Figure 8). It seems that most ribbed moraines take around 100 years to grow and migrate 1 km downstream, approximately two wavelengths. Our caveats, mentioned earlier, with regard to not knowing the true probability density function of the parameters also applies to these estimates.

8.5. Is There any Physical or Empirical Support for the Modeled Sensitivities of Wavelength Prediction to the Governing Parameters?

[48] Figure 9 illustrates the sensitivity of predicted wavelength to the five governing parameters. For each value of a parameter, a wavelength frequency distribution is computed, and bins are plotted as a function of the parameter and wavelength. Variation in the modal wavelength with the parameter values indicates sensitivity.

[49] For ice with a linear rheology, *Fowler* [2000] predicts that the wavelength of maximum growth rate varies with the square root of ice viscosity, till rate factor *A,* and

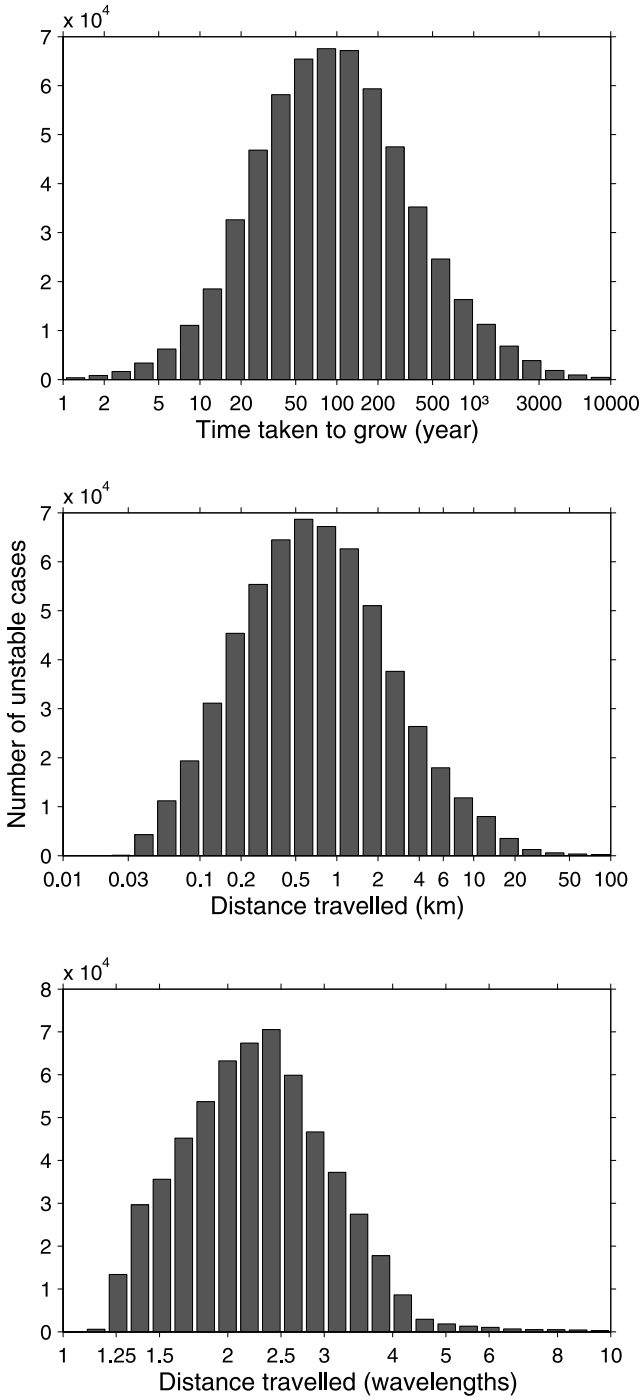

Figure 8. Histograms of populations of predicted (top) growth time, (middle) distance traveled measured in km during this growth time, and (bottom) distance traveled measured in wavelengths. Growth phase is defined as period from when the relief is 100 mm (a typical depth of deformation) to 20 m (a typical ribbed moraine amplitude).

the effective pressure. In our model we do not prescribe the till rate factor, but implicitly define it through our choices of velocity, shear stress and effective pressure. However, all else being equal, the till rate factor is proportional to the velocity, so we expect the wavelength to be proportional to the square root of the velocity for a linear ice rheology, and this evidently also holds for a nonlinear ice rheology (Figure 9). Since basal shear stress affects ice viscosity through the Glen relationship, we expect there to be a direct dependence on shear stress, which is also clearly demonstrated (Figure 9). There are also clear dependencies on effective pressure and till thickness. There is no strong dependence on the rheological index *b*.

[50] Circumstantial observations indicate that ribbed moraine wavelength appears to vary with till thickness [*Hättestrand*, 1997] and when a field crosses from one bedrock lithology to another where permeability is different [*Clark and Meehan*, 2001]. Such changes could provide useful checks on model functioning. This approach has yet to be tackled properly, because the observations have not been systematically compiled, but we report two circumstances where model predictions and data can be reasonably compared. In county Monaghan Ireland, the field of megascale ribbed moraine reported by *Clark and Meehan* [2001] exhibit an increase in wavelength across the boundary from well-drained Carboniferous limestone just northwest of Monaghan town to less permeable Ordovician shale, sandstone, basalt and rhyolite that dominate the landscape to the southeast. If a substantial proportion of ice sheet drainage is being carried in the aquifer we can infer that effective pressure decreased across this boundary. According to model predictions (Figure 9) as effective pressure decreases then wavelength should increase. This direction of change is consistent with the observations. However, we consider this a weak test because as effective pressure changes then this would most likely have influenced other parameters such as ice velocity and shear stress and we have not yet accounted for these.

[51] In a discussion of minor ribbed moraine, *Hättestrand* [1997] comments that the short-wavelength features are mostly found on high ground where the till cover is evidently much thinner in comparison with the longer-wavelength features found on valley floors where the till is thick. BRIE indicates (Figure 9) that as till thickness decreases then wavelength should also decrease, and again this is consistent with the limited observations available. Future compilations of ribbed moraine wavelength and spatial variation coincident with changes in bedrock permeability, till thickness etc should permit more rigorous model testing especially when BRIE is coupled to an ice sheet model so we can model concomitant changes in all governing parameters.

9. Conclusions

[52] A physically based model for ribbed moraine formation (BRIE) based on a naturally arising instability in the coupled flow of ice and subglacial sediment, has been explained and its predictions tested against a large database describing the spatial properties of these landforms. We conclude that this specific instability mechanism and its model formulation in BRIE correctly produce the patterning of ribbed moraines; that of a dominant downstream wavelength and unbounded lateral wavelength yielding transverse waves (i.e., ridges) with a preferred wavelength.

[53] We have compared the wavelength predictions of the model with observed wavelengths of ribbed moraine fields

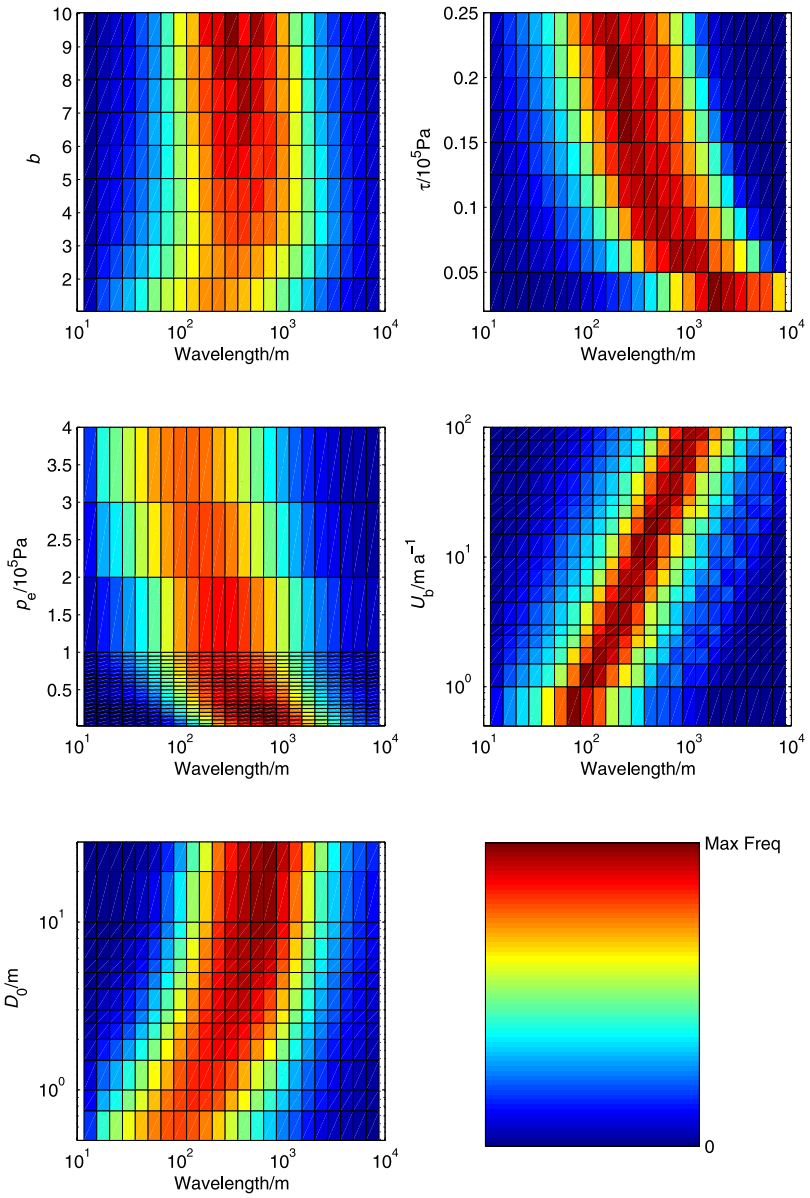

Figure 9. Histograms of frequency of occurrence of predicted wavelength plotted as a function of one of the parameters being varied (indicated on *y* axis). Colors are scaled by maximum frequency in each variable case. These examples are for the reduced parameter set. Note weak sensitivity for rheological index *b* and strong sensitivity for velocity (*Ub*). Color coding shown at bottom right.

[*Dunlop and Clark*, 2006a] but care is required in drawing conclusions from this exercise because the physical conditions (parameter values) of ribbed moraine formation are not well known. An attempt to circumvent this problem was made by defining glaciologically plausible ranges for the physical parameters which determine the wavelength of maximum growth rate in the BRIE model, and assuming that all the observed ribbed moraines were formed under this range of conditions. The model predicts ribbed moraine formation at order of magnitude wavelengths between 100 and 1000 m which we interpret as a major accomplishment of the model. Our bed ribbing instability may have produced completely unrealistic wavelengths such as 10–1000 km, from which we would have concluded with falsification. Unsurprisingly however, given the large range of the input parameters, the model predictions produced a range of wavelengths somewhat broader than those observed in nature. This is likely to be a consequence of the range of input parameters being broader than those under which ribbed moraine actually form. Thus, one cannot say that BRIE has been falsified on account of its slight overpredictions of ribbed moraine formation at short and long wavelengths.

[54] Model computations of the rate of growth of small bumps into landforms of ribbed moraine amplitude indicates a plausible time (mode of 100 years) for their formation, when compared with the limited expectations and observations regarding real subglacial bedform growth. Given that the theory requires bumps to migrate downstream as they grow, an important consideration was to

check that they could grow to sufficient relief prior to being migrated out of the subglacial environment. This condition is easily satisfied and with typical migration distances of 1 to 100 m and a maximum of 10 km.

[55] The model predicts different wavelengths for different conditions of till thickness and bed drainage (via effective pressure). Variations of wavelength of real ribbed moraine with varying till thickness (in Sweden) and bed drainage (in Ireland) are reported, and we note that the model predictions are at least in principle consistent with this variation, in that they vary in the right direction.

[56] Although the heritage of the BRIE approach comes from a school of thought that regards the rheology of subglacial sediment to approximate that of a viscous fluid, we found that the model was not sensitive to the rheological exponent and that instabilities are equally well predicted under a viscous through to plastic medium. This is a significant conclusion, although it means that landscape formation may well be unilluminating about some aspects of the ice stream basal boundary.

[57] This paper has considered geomorphic features that emerge spontaneously from a uniform till cover. Nearly always, landforms are inherited. However, the instability mechanism discussed here is expected to operate on a nonuniform till cover, and will eventually shape it into a form where the original structure is no longer apparent. While this is happening, we believe the new landforms will be a palimpsest on the old forms. Modeling is currently being undertaken to confirm this conjecture.

[58] In summary, our tests failed to falsify the model, and the BRIE theory remains a viable candidate for explaining ribbed moraine formation. The problems faced in this paper regarding the verification of BRIE stem from our ignorance of the physical conditions under which ribbed moraine form. The successes of the BRIE theory are that it predicts the occurrence of ribbed moraine pattern, and quantitatively predicts ribbed moraine of appropriate wavelengths. It remains to be seen whether quantitative formulations of the other theories can achieve the same success.

[59] **Acknowledgments.** The authors would like to thank Dave Evans and an anonymous reviewer for their comments on this manuscript. This work was supported by NERC grant NE/D011175/1 ''Testing the Instability Theory of Subglacial Bedform Production.'' This paper is dedicated to Brien Dunlop for his support during visits to the British Antarctic Survey.

References

Alley, R. B., D. D. Blankenship, S. T. Rooney, and C. R. Bentley (1989), Water-pressure coupling of sliding and bed deformation: III. Application to Ice Stream B, Antarctica, *J. Glaciol.*, *35*, 130–139.

Ashton, A., A. B. Murray, and O. Arnoult (2001), Formation of coastline features by large-scale instabilities induced by high-angle waves, *Nature*, *414*, 296–300, doi:10.1038/35104541.

Aylsworth, J. M., and W. W. Shilts (1989), Bedforms of the Keewatin Ice Sheet, Canada, *Sediment. Geol.*, *62*, 407–428, doi:10.1016/0037-0738(89)90129-2.

Beskow, G. (1935), Patriska och kvartärgeologiska resultat av grusinventeringen I Norrbottens län, *Geol. Foeren. Stockholm Foerh.*, *57*, 120–123.

Blatter, H. (1995), Velocity and stress-fields in grounded glaciers—A simple algorithm for including deviatoric stress gradients, *J. Glaciol.*, *41*(138), 333–344.

Bouchard, M. A. (1989), Subglacial landforms and deposits in central and northern Québec, Canada, with emphasis on Rogen moraines, *Sediment. Geol.*, *62*, 293–308, doi:10.1016/0037-0738(89)90120-6.

Boulton, G. S. (1987), A theory of drumlin formation by subglacial deformation. In *Drumlin Symposium*, eds J. Menzies and J. Rose, Balkema, Rotterdam, 25–80.

Clark, C. D., and R. Meehan (2001), Subglacial bedform geomorphology of the Irish Ice Sheet reveals major configuration changes during growth and decay, *J. Quaternary Sci.*, *16*, 483–496, doi:10.1002/jqs.627.

Dunlop, P. (2004), The Characteristics of ribbed moraine and assessment of theories for their genesis, Ph.D. thesis, 363 pp., Univ. of Sheffield, Sheffield, U. K.

Dunlop, P., and C. D. Clark (2006a), The morphological characteristics of ribbed moraine, *Quat. Sci. Rev.*, *25*, 1668–1691, doi:10.1016/j.quascirev.2006.01.002.

Dunlop, P., and C. D. Clark (2006b), The distribution of ribbed moraines in the Lac Naococane region, central Quebec, Canada, *J. Maps*, 56–67.

Drazen, P. G. (2002), *Introduction to Hydrodynamic Stability*, Cambridge Univ. Press, Cambridge, U. K.

Dyke, A. S., T. F. Morris, D. E. C. Green, and J. England (1992), Quaternary geology of Prince of Wales Island, arctic Canada, *Geol. Surv. Can. Mem. Ser.*, vol. 433, Geol. Surv. of Can., Ottawa, Ont.

Elbelrhiti, H., P. Claudin, and B. Andreotti (2005), Field evidence for surface-wave-induced instability of sand dunes, *Nature*, *437*, 720–723, doi:10.1038/nature04058.

Fisher, T. G., and J. Shaw (1992), A depositional model for Rogen moraine, with examples from the Avalon Peninsula, Newfoundland, *Can. J. Earth Sci.*, *29*, 669–686.

Fowler, A. C. (2000), An instability mechanism for drumlin formation, in *Deformation of Glacial Materials*, *Spec. Publ. Geol. Soc. Ser.*, vol. 176, edited by A. Maltman, M. J. Hambrey, and B. Hubbard, pp. 307–319, Geol. Soc. of Am., Boulder, Colo.

Frödin, G. (1913), Bidrag till västra Jämtlands senglaciala geologi, *Sver. Geol. Unders. Ser. C*, *246*, 1–236.

Frödin, G. (1925), Studien über die Eissheide in Zentralskandinavien, *Bull. of the Geol. Inst. at Univ. Upsala*, *19*, 129–214.

Getling, A. V. (1997), *Rayleigh-Bénard Convection Structures and Dynamics*, *Adv. Ser. Nonlinear Dyn.*, vol. 11, World Sci., London.

Hättestrand, C. (1997), Ribbed moraines in Sweden—Distribution pattern and palaeoglaciological implications, *Sediment. Geol.*, *111*, 41–56, doi:10.1016/S0037-0738(97)00005-5.

Hättestrand, C., and J. Kleman (1999), Ribbed moraine formation, *Quat. Sci. Rev.*, *18*, 43–61, doi:10.1016/S0277-3791(97)00094-2.

Hersen, P., K. H. Andersen, H. Elbelrhiti, B. Andreotti, P. Claudin, and S. Douady (2004), Corridors of barchan dunes: Stability and size selection, *Phys. Rev. E*, *69*, 1–12.

Hindmarsh, R. C. A. (1997), Deforming beds: Viscous and plastic scales of deformation, *Quat. Sci. Rev.*, *16*, 1039–1056, doi:10.1016/S0277-3791(97)00035-8.

Hindmarsh, R. C. A. (1998a), The stability of a viscous till sheet coupled with ice flow, considered at wavelengths less than ice thickness, *J. Glaciol.*, *44*, 288–292.

Hindmarsh, R. C. A. (1998b), Drumlinization and drumlin-forming instabilities: Viscous till mechanisms, *J. Glaciol.*, *44*, 293–314.

Hindmarsh, R. C. A. (1998c), Ice-stream surface texture, sticky-spots, waves and breathers: The Couples flow of ice, till and water, *J. Glaciol.*, *44*, 589–614.

Hindmarsh, R. C. A. (1999), Coupled ice-till dynamics and the seeding of drumlins and bedrock forms, *Ann. Glaciol.*, *28*, 221–230, doi:10.3189/172756499781821931.

Högbom, A. G. (1920), Geologisk Beskrivning Over Jemtlands Län, 2nd ed., *Sver. Geol. Unders. Ser. C*, vol. 140, Redins Antikvariat, Uppsala, Sweden.

Hoppe, G. (1952), Hummocky moraine regions, with special reference to the interior of Norrbotten, *Geogr. Ann.*, *41A*, 193–212.

Hutter, K. (1983), *Theoretical Glaciology*, D. Riedel, Dordrecht, Netherlands.

Jackson, M., and B. Kamb (1997), Marginal shear stress of ice stream B, *J. Glaciol.*, *43*, 415–426.

Joughin, I., W. Abdalati, and M. Fahnestock (2004), Large fluctuations in speed on Greenland's Jakobshavn Isbrae glacier, *Nature*, *432*(7017), 608–610, doi:10.1038/nature03130.

Knight, J., and A. M. McCabe (1997), Identification and significance of ice-flow transverse subglacial ridges (Rogen moraines) in northern central Ireland, *J. Quaternary Sci.*, *12*(6), 519–534, doi:10.1002/(SICI)1099-1417(199711/12)12:6<519::AID-JQS313>3.0.CO;2-Q.

Komarova, N. L., and S. J. M. H. Hulscher (2000), Linear instability mechanisms for sand wave formation, *J. Fluid Mech.*, *413*, 219–246, doi:10.1017/S0022112000008429.

Kurimo, H. (1977), Patterns of dead-ice deglaciation forms in western kemijärvi, northern Finland, *Fennia*, *153*, 43–56.

Kurimo, H. (1980), Depositional deglaciation forms as indicators of different glaciomarginal environments, *Boreas*, *9*, 179–191.

Lundqvist, J. (1951), Beskrivning Till Jordartskarta Över Kopparbergs Län, *Sver. Geol. Unders. Ser. C*, vol. 21, Redins Antikvariat, Uppsala, Sweden.

Lundqvist, J. (1969), Problems of the So-Called Rogen Moraine, *Sver. Geol. Unders. Ser. C*, vol. 648, Redins Antikvariat, Uppsala, Sweden.

Lundqvist, J. (1989), Rogen (ribbed) moraine: Identification and possible origin, *Sediment. Geol.*, *62*, 281–292, doi:10.1016/0037-0738(89)90119-X.

Lundqvist, J. (1997), Rogen moraine—An example of two-step formation of glacial landscapes, *Sediment. Geol.*, *111*, 27–40, doi:10.1016/S0037-0738(97)00004-3.

Mannerfelt, C. (1945), Några glacialgeologiska formelement och deras vittnesbörd om inlandsisens avsmältningsmekanik I svensk och norsk fjällterräng, *Geogr. Ann.*, *27A*, 1–239.

Minell, H. (1977), Transverse moraine ridges of basal origin in Härjedalen, *Geol. Fören. Stockholm Förh.*, *99*, 271–277.

Minell, H. (1980), The distribution of local bedrock material in some moraine forms from the inner part of northern Sweden, *Boreas*, *9*, 275–281.

Möller, P. (2006), Rogen moraine—An example of glacial reshaping of pre-existing landforms, *Quat. Sci. Rev.*, *25*, 362–389, doi:10.1016/j.quascirev.2005.01.011.

Nye, J. F. (1969), A calculation on the sliding of ice over a wavy surface using a Newtonian viscous approximation, *Proc. R. Soc. London Ser. A*, *311*(1506), 445–467.

Paterson, W. S. B. (1994), *The Physics of Glaciers*, 3rd ed., Pergamon, Oxford, U. K.

Philips, J. D. (1993), Instability chaos in hillslope evolution, *Am. J. Sci.*, *283*, 25–48.

Prest, V. K., D. G. Grant, and V. N. Rampton (1968), Glacial map of Canada, *Map 1253A*, scale 1:5,000,000, Geol. Surv. of Can., Ottawa, Ont.

Rose, J. (1989), Glacier stress patterns and sediment transfer associated with the formation of superimposed flutes, *Sediment. Geol.*, *62*(2–4), 151–176.

Sarala, P. (2006), Ribbed moraine stratigraphy and formation in southern Finnish Lapland, *J. Quaternary Sci.*, *21*(4), 387–398, doi:10.1002/jqs.995.

Schoof, C. (2007), Pressure-dependent viscosity and interfacial instability in coupled ice-sediment flow, *J. Fluid Mech.*, *570*, 227–252, doi:10.1017/S0022112006002874.

Sharp, D. H. (1984), An overview of Rayleigh-Taylor instability, *Physica D*, *12*(1–3), 3.

Shaw, J. (1979), Genesis of the Sveg till and Rogen moraines of central Sweden: A model of basal melt out, *Boreas*, *8*, 409–426.

Shilts, W. W. (1977), Geochemstry of till in perennially frozen terrain of the Canadian shield—Application to prospecting, *Boreas*, *6*, 203–212.

Smalley, I., and J. Warburton (1994), The shape of drumlins, their distribution in drumlin fields, and the nature of the sub-ice shaping forces, *Sediment. Geol.*, *91*, 241–252, doi:10.1016/0037-0738(94)90132-5.

Smith, A. M., T. Murray, K. W. Nicholls, K. Makinson, G. Aðalgeirsdóttir, A. E. Behar, and D. G. Vaughan (2007), Rapid erosion, drumlin formation and changing hydrology beneath an Antarctic Ice Stream, *Geology*, *35*, 127, doi:10.1130/G23036A.1.

Stokes, C. R., and C. D. Clark (2001), Palaeo-ice streams, *Quat. Sci. Rev.*, *20*, 1437–1457.

Stokes, C., C. D. Clark, O. B. Lian, and S. Tulaczyk (2006), Geomorphological map of ribbed moraines on the Dubawnt Lake palaeo-ice stream bed: A signature of ice stream shut-down?, *J. Maps*, 1–9.

Wattenson, L. (1983), Rogen-Myskelsjöområdet, in *Funäsdalen: Description and Assessment of Areas of Geomorphological Importance*, edited by I. Borgström, *Geomorphological Map 17C*, pp. 25–32, Statens Naturvårdsverk, Stockholm.

Whillans, I. M., and C. J. Van der Veen (1993), Patterns of calculated basal drag on ice streams B and C, Antarctica, *J. Glaciol.*, *39*, 437–446.

Yamamoto, M. K., M. Fujiwara, T. Horinouchi, H. Hashiguchi, and S. Fukao (2003), Kelvin-Helmholtz instability around the tropical tropopause observed with the Equatorial Atmosphere Radar, *Geophys. Res. Lett.*, *30*(9), 1476, doi:10.1029/2002GL016685.

C. D. Clark, Department of Geography, University of Sheffield, Sheffield S10 2TN, UK. (c.clark@sheffield.ac.uk)

P. Dunlop, School of Environmental Sciences, University of Ulster, Room G263, Cromore Road, Coleraine BT52 1SA, UK. (p.dunlop@ulster.ac.uk)

R. C. A. Hindmarsh, Physical Science Division, British Antarctic Survey, Natural Environment Research Council, High Cross, Madingley Road, Cambridge CB3 0ET, UK. (rcah@bas.ac.uk)